# Multi-instrument STIX microflare study


J. Saqri[1], A. Veronig[1], E.C.M. Dickson[1,2] A. Warmuth[3] , A. F. Battaglia[2,4], S. Krucker[2,5], M. Battaglia[2], H. Xiao[2] , G. Hurford[2] and the STIX Team

[1]Institute of Physics, University of Graz
[2]University of Applied Sciences and Arts Northwestern Switzerland
[3]Leibniz-Institut für Astrophysik Potsdam (AIP)
[4]ETH Zürich
[5]Space Sciences Laboratory, University of California


## Introduction

Solar flares are generally thought to be the impulsive release of magnetic energy giving rise to a wide range of solar phenomena that influence the heliosphere and in some cases even conditions on earth.
During its commissioning phase in 2020, the Spectrometer/Telescope for Imaging X-rays (STIX) on board the Solar Orbiter (SOLO) spacecraft clearly observed 26 microflares and demonstrated its capability to reconstruct spectra and imaging for larger (GOES B class and larger) events(Battaglia et. al., 2021). In this study, we make use of these capabilities to perform flare plasma diagnostics for a well observed B6 event which has the best count statistics in this set of commissioning flares (see right panel of Fig.1) . We further investigated a flare of GOES class B2 which is the smallest event from this set with a sufficient countrate for spectral analysis (left side of Fig.1). As there is only limited data from other SOLO instruments available to complement these initial observations, we make use of observations from GOES and instruments onboard the SDO spacecraft to complement the STIX instrument. The SDO/AIA instrument provides high resolution, high cadence EUV imaging that additionally allows to reconstruct the Differential Emission Measure (DEM) of the thermal flare plasma while GOES provides an spatially integrated measurement in two X-ray channels that can be used for plasma diagnostics.

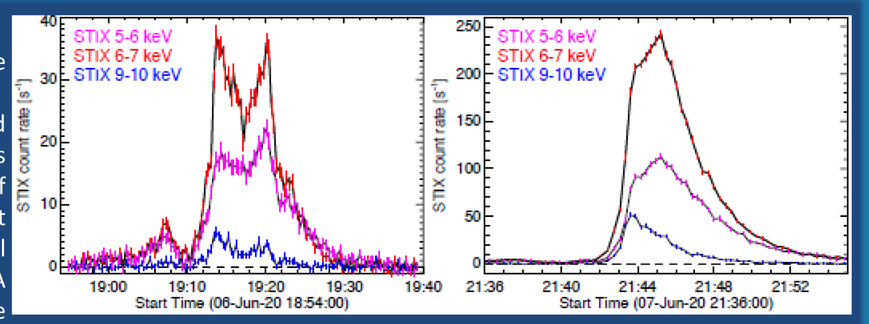


*Figure 1: STIX Lightcurves (Battaglia et. al., 2021).*

## Results

### B6 flare on June 7

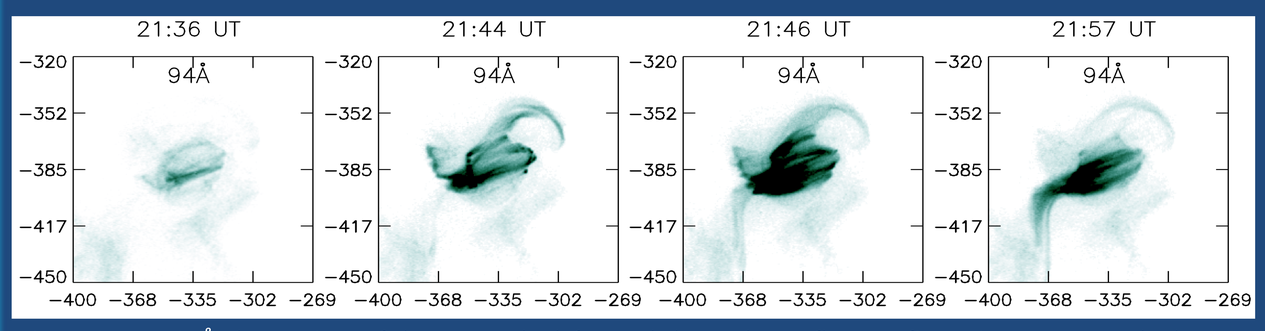


*Figure 2: AIA 94Å observations of the event. The left panel shows the preflare configuration. Later panels show loops filled by hot plasma*

Figure 2 shows the evolution of the thermal plasma as seen in the AIA 94Å filter. It adds imaging information to the spatially integrated STIX lightcurves shown in Fig. 1.
Compared with the pre event level shown in the leftmost panel of Fig. 2, it shows the filling of the loops by heated plasma at 21:44 UT, a further increase at 21:46 and the cooling of the hot plasma at 21:57 UT.
To quantify the change in plasma temperature and density, the DEM of the flaring region is analyzed in Figures 3 and 4. DEMs were reconstructed using a SSWIDL code available in the literature (Hannah and Kontar, 2012). In Fig. 3 flare loops and kernels are identified based on 94 and 171Å background subtracted images shown in the top panel. The selected regions are overploted with the masks and curves in blue, showing the flare loops and red and green indicating the flare kernels on the left and right. The time evolution of the DEM profile averaged over the flare loop mask is plotted in the left panels in blue. It reveals that the loops initially fill with hot plasma as the DEM is centered roughly around 7MK at 21:48 UT. At 21:52, a cooler component centered around 3MK develops as the initially hot plasma cools down. By 21:57, most of the plasma in the flare loops has cooled down to around 3MK as seen in the left bottom panel. The DEM profile of the right flare kernel shown in green in the rightmost panel shows a 3MK peak present over the entire duration. The left kernel in the middle panel also exhibits this 3MK peak, as well as the initially hot 7MK component that later cools down as loops are present along the line of sight between the observer and the flare kernel. This difference in temperature of the thermal plasma in the flare loops and flare kernels is further illustrated in Fig. 4.

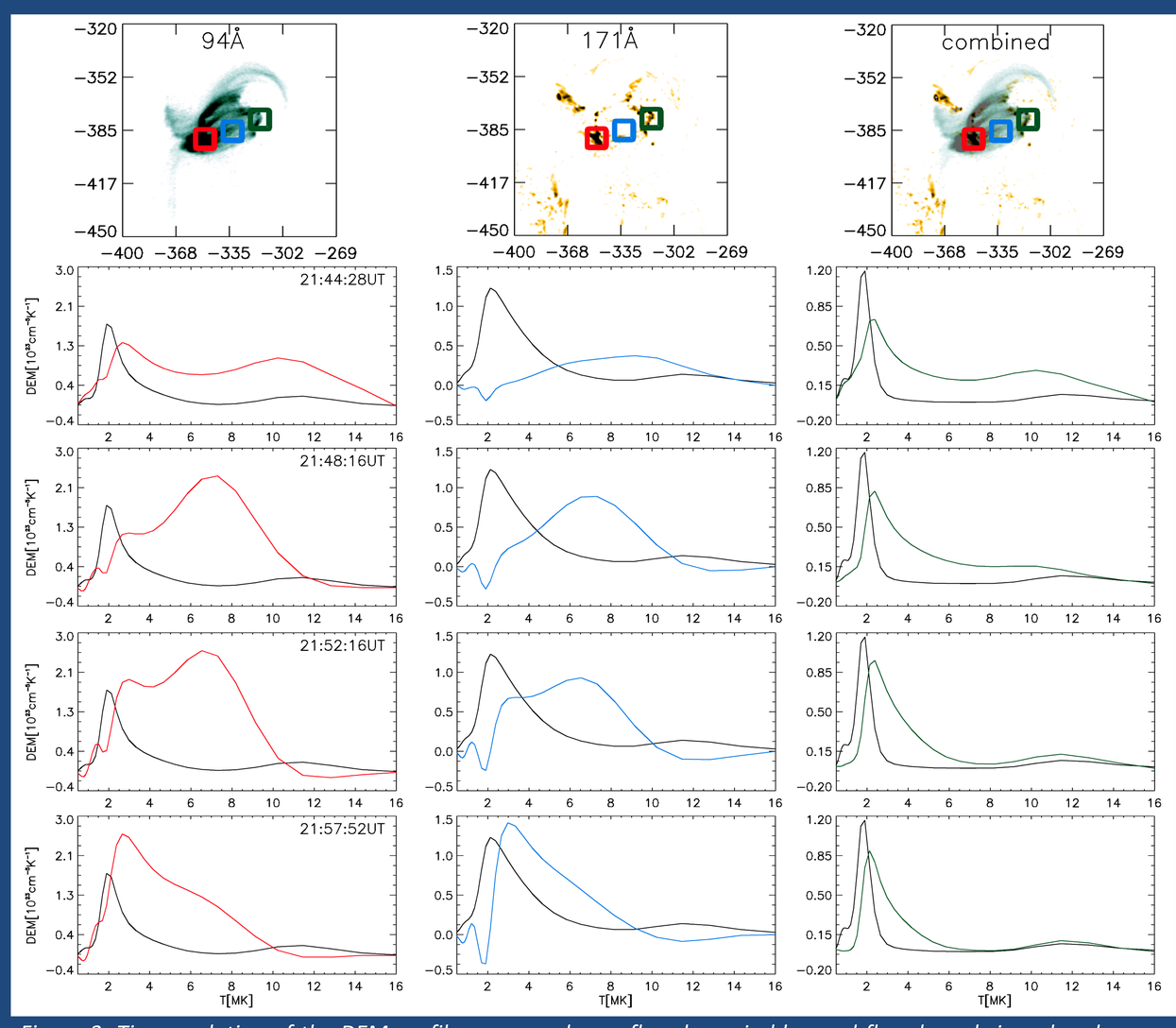


*Figure 3: Time evolution of the DEM profiles averaged over flare loops in blue and flare kernels in red and green. Shown in black is the pre event background.*

Fig. 4 shows the total Emission Measure (EM) integrated from 0.5 to 4 MK on the left side and from 4 to 10 MK on the right for four distinct times during the flare event. In the top row at 21:44 UT and at 21:48 the cooler EM bin on the left clearly shows the flare kernels while the hotter bin shown on the right shows the hot plasma in the loops. At 21:52 and more pronounced at 21:57 the flare loops can now also be seen in the 0.5-4 MK bin while there is less EM in the hot 4.5-10MK bin compared to 21:48 as the thermal plasma in the loops cools down.

The results from the DEM reconstructed from AIA EUV data are combined with STIX and GOES observations in Fig. 5.
Spectral fitting of the STIX spectra reveals the presence of a nonthermal component at the begining of the event between 21:42 and 21:45 UT (bottom panels). The three top panels show the temperature,EM and thermal energy derived from STIX, GOES and the AIA DEM. The absolute values and timing differ due to the different instrument characteristics. STIX is only sensitive thermal plasma above 10MK while the AIA DEM images plasma down to 0.5 MK which brings the average plasma temperature down. The GOES SXR instrument lies in between those two extremes resulting in derived temperatures for the thermal flare plasma that lie between these two extremes.

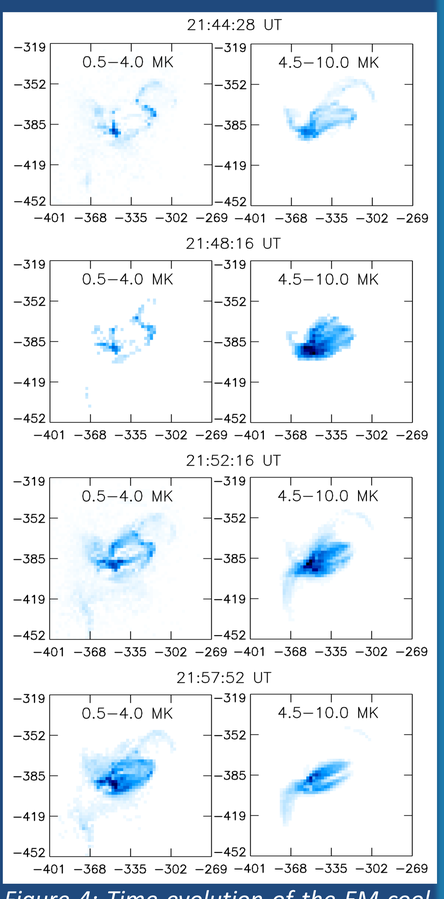


*Figure 4: Time evolution of the EM cool and hot temperature bins.*

### B2 flare on June 6

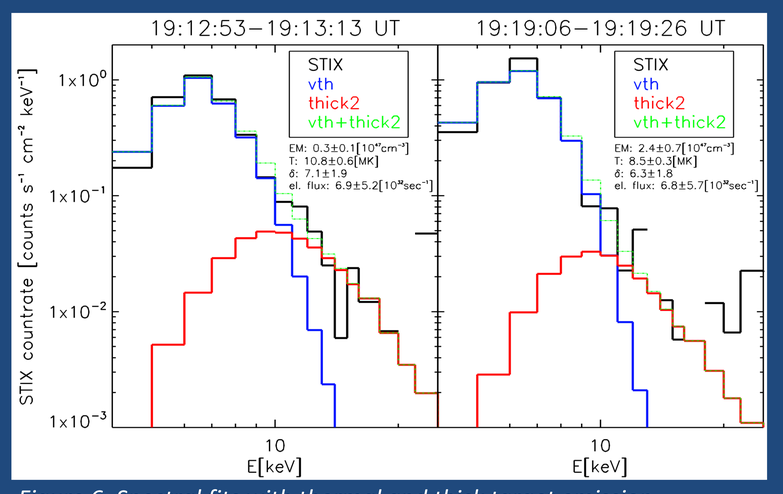


*Figure 6: Spectral fits with thermal and thick target emission.*

On June 6 2020, a GOES B2 flare was observed that shows a distinct double peaked shape in the STIX lightcurves (Fig.1). Using a 20 second time integration, the recorded counts are high enough to allow spectral fitting. During both peaks in the STIX lightcurve, the best fits are achieved using the sum of a isothermal and a non thermal thick target component (see Fig.6). While the uncertainties are quite large, lightcurves from the AIA 1600Å channel from the different regions indicated on the left side of Fig. 7 show that the chromospheric response indeed coincides with the nonthermal energy input

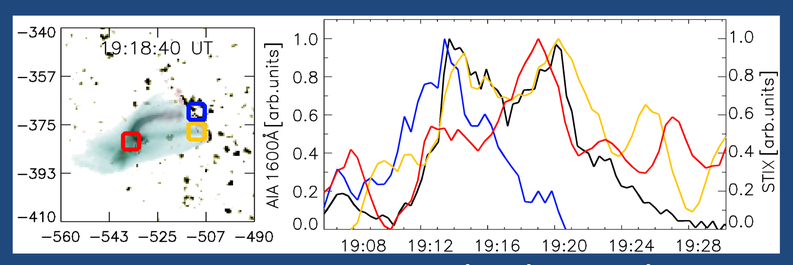


*Figure 7: Left: Composite image of AIA 94Å,211Å and 1600Å. Right: Lightcurves of the chromospheric response seen in the AIA 1600Å channel from the regions indicated on the left.*

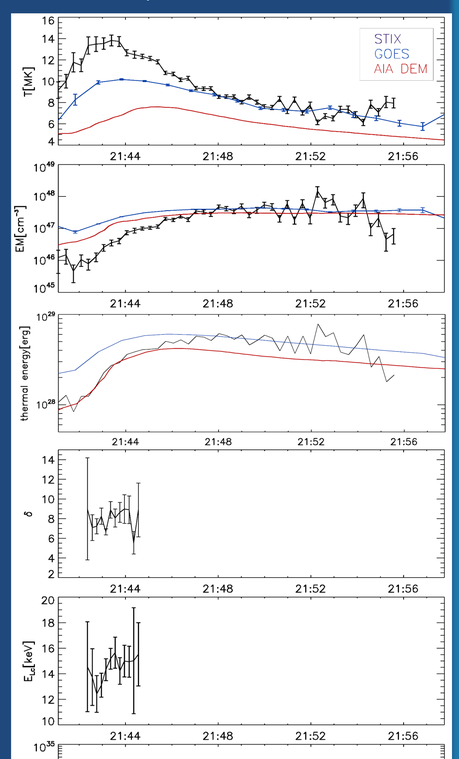


*Figure 5: Top panels: Time evolution of temperature, EM and thermal energy of the flaring plasma derived from STIX, GOES and DEM from AIA data. Bottom panels: Evolution of the parameters for the best spectral fits to the STIX spectrum assuming a combination of thermal and thick target bremsstrahlung.*

## Discussion

Combining the results from STIX spectroscopy, DEM analysis and GOES filter ratios allows for comparing the evolution of derived EM and ''isotermal'' temperature from each instrument (Fig.4). The derived values vary between the methods due to the different instrument characteristics. As STIX is only sensitive to hot (>10MK) thermal plasma, additional information about cooler flare plasma can be inferred with GOES and AIA data if simultaneous observations are possible. It is demonstrated that the high spatial resolution, high cadence AIA EUV data and the DEM reconstructed from the data are valuable tools to complement observations from the STIX X-ray instrument as they allow to distinguish the different components of the multi-thermal flare plasma (e.g. flare kernels and loops) and to observe flare plasma outside the sensitivity range of X-ray instruments. The study of the June 6 flare further showed that STIX can detect nonthermal emission at least down to GOES class B2. The capabilities demonstrated here will be very usefull when Solar Orbiter enters its nominal science phase towards the end of 2021.

## References


Differential emission measures from the regularized inversion of Hinode and SDO data, I. G. Hannah, E. P. Kontar, A&A 539 A146
STIX X-ray microflare observations during the Solar Orbiter commissioning phase, Battaglia et. al., in press